Research

iMedPub Journals
www.imedpub.com

Nano Research & Applications
ISSN 2471-9838

2022
Vol.8 No.7:86

Antimicrobial and Detoxification Study of Novel Luminescent CuO Nanoparticles Synthesized By White Garland Lily Leaves Extract

K G Mane*, P B Nagore, A J Ghoti and A P Salve

Department of Chemistry, University of Mumbai, Doshi Vakil Arts College and G.C.U.B. Sci. & Comm. College, Maharashtra, India

***Corresponding author:** K G Mane, Department of Chemistry, University of Mumbai, Doshi Vakil Arts College and G.C.U.B. Sci. & Comm. College, Maharashtra, India, E-mail: kanchanmane13@gmail.com

Received date: June 17, 2022, Manuscript No. Ipnto-22-13800; **Editor assigned date**: June 20, 2022, PreQC No. Ipnto-22-13800 (PQ); **Reviewed date**: June 27, 2022, QC No. Ipnto-22-13800; **Revised date**: July 08, 2022, Manuscript No. Ipnto-22-13800 (R); **Published date**: July 18, 2022, DOI: 10.36648/2471-9838.8.7.86

Citation: Mane KG, Nagore PB, Ghoti AJ, Salve AP (2022) Antimicrobial and Detoxification Study of Novel Luminescent CuO Nanoparticles Synthesized By White Garland Lily Leaves Extract. Nano Res Appl Vol. 8 No.7:86

Abstract

The novel luminescent copper oxide nanoparticles were furnished by using white garland lily leaves extract. The method for this synthesis was economical, simple, environment friendly, and importantly followed green chemistry principles for the development of a proficient approach in the arena of biological applications and detoxification of industrial-grade toxic dye. The characterization study of CuONPs was done by UV-Visible, FT-IR, XRD, HRTEM, FESEM-EDAX and PL spectra. The particle size (average) revealed by XRD, HRTEM and FESEM analysis was 40±0.5 nm. The O.D. around 300 nm in UV-Vis. spectra established the effective synthesis of CuONPs while the peaks around 295 nm and 590 nm in PL spectra revealed its luminescence property. The novel CuONPs were verified against the selected bacterial and fungal strains. The CuONPs exhibited outstanding antibacterial activities *vs E. coli* and *S. Pyogenus* while having considerable antifungal activities against selected fungal strains.

Moreover, the CuONPs were tested for photocatalytic degradation proficiency against Methylene Blue (MB) and found effective even after three cycles (100 % removal in 70 min). The photocatalytic efficacy and its high reusability in consort with great adaptability of economic green synthesis favor the practice of novel CuONPs as a hopeful choice for the detoxification of natural resources poisoned with industrial dye.

Keywords: Green method; Nanotechnology; White garland lily; Plant leaves.

Introduction

The present epidemic has asked for an urgent alternative to search for human Anti-Microbial Resistance (AMR) and the cleaning of natural resources. Unfortunately, the AMR has emerged as a severe threat as the microbes show mutations, leading to the failure of existing antimicrobial agents, causing huge loss of human lives with economy [1,2].

Nowadays, Nanotechnology and Nanoscience have arisen as the future technology for life. Researchers worldwide are working on the enrichment of the nanoworld. In that context, people are working on newer nanoparticle synthesis methods apart from existing methods.

Biological methods, especially using plants and secondary metabolites for nanoparticle synthesis, have been the budding area for researchers worldwide owing to many benefits over existing methods [3-7].

Copper, a metal of the first transition series, is a key element for the kingdom animalia. There we find ample studies on the phytofabrication of CuONPs [8-14]. White garland lily, also called ginger lily (Figure 1), is a plant from the family Zingiberaceae and is a perennial ornamental species known for its beautiful white flowers used as garland flowers in Maharashtra. *Hedychium coronarium Koenig* is the botanical name of this species.

It has some significant medicinal properties like antimicrobial, antioxidant, anti-hypertensive, and antimalarial potentials [15,16]. This article presents an eco-benevolent, simple phytofabrication of CuONPs employing White Garland Lily Leaves Extract (WGLLE), its antibacterial and antifungal activities along with its photocatalytic efficacy.

To date this plant is being utilized only for AgNP synthesis, using rhizome extract. So, this article devotes the phytosynthesis of CuONPs with WGLLE, for the first time.

Figure 1: White garland lily plant.

Experiment

Materials

CuSO4.5H2O (AR grade), NaHCO3 (AR grade), and other chemicals were purchased from Molychem, Mumbai, India, and utilized as such.

Plant recognition and WGLLE preparation

The plant recognition was done by Mr. Amol Salve, based on its characteristics explained in Flora of Maharashtra [17]. The specimen was submitted to the Botany department. Freshly collected leaves (20 g) were carried from a household plot belonging to Mr. Satish Doshi, a retired headmaster located at Goregaon. Then leaves were washed in the laboratory, first by tap water followed by double distilled water to remove worthless material, and then sliced into very fine bits. These bits were transferred into a 250 ml beaker for boiling, containing 200 ml double distilled water for an hour using a hot plate. After an hour mixture was double filtered by ordinary and then by Whatman paper no.1 to get White Garland Lily Leaves Extract (WGLLE). The WGLLE was stored in a refrigerator till further use.

Synthesis of CuONPs

The freshly made 0.1M CuSO4.5H2O solution with pH 4.6 was mixed to WGLLE in 1:4 ratios, obtained after optimization, which led to an instant alteration in color from green to dark green, which further turned black after stirring on a magnetic stirrer for the 50 minutes at 500 RPM. The black-colored solid received was then centrifuged at 3500 RPM for around 45 min. After that, it was exposed for combustion in a muffle furnace at around 450°C. Finally, it was gathered and preserved in a sample tube until further use at the final stage (Figure 2).

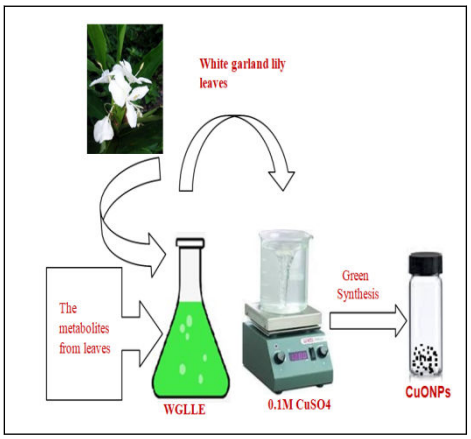

Figure 2: Diagrammatic representation-Synthesis of CuONPs.

Characterization techniques

The UV–Vis. spectrum of CuONPs was recorded by spectrophotometer (Model-JASCO V-770). Functional groups and chemical composition were analyzed by FT-IR (4600 Type A D044761786) while PL spectra was recorded by spectrofluorometer (Model No. FP-8200, Sr.No-C026661448). The XRD spectra were recorded by X-ray diffractometer (XRD, Bruker, D8-Advanced Diffractometer) using Cu-Kα radiation (λ =0.154 nm) at 40 kV and 40 mA in the range 10-80°. High-resolution transmission microscopy analysis was carried out with Model-JEM 200 F, Accelerating potential: 120 kV and 200 kV. The HRSEM-EDS (FEI Quanta, FEG-200) was used to record the exact size, shape, and elemental composition of CuONPs.

Phytochemical screening

The active phytometabolites present in WGLLE were investigated following standard protocols [18].

Antibacterial activities

The Broth dilution method was used to evaluate the antibacterial efficacy of CuONPs [19] with diluent as DMSO [20,21]. Two G +ve and two G –ve bacteria were tested in the experiment. The MIC was taken to the concentration which showed at least 99% inhibition. The results are displayed after triplicate analysis.

Antifungal activities

The CuONPs were evaluated *vs* particular fungal strains using agar dilution protocol following Wiegand *et al.* [19]. The MIC was considered to be the concentration displaying minimum 99% inhibition with Griseofulvin and Nystatin as reference drugs. The results were tabulated after triplicate analysis.

Detoxification study

This was carried out with MB dye. The 0.25 gm of CuO photocatalyst was dispersed in different concentrations of dye used *viz*., 1000, 750, 500, 250 ppm and stirred in dark for half an hour to achieve the adsorption-desorption equilibrium mechanism. Then, the solution was exposed to solar radiation and O.D. was recorded every 10 min.

Results and Discussion

The Structural and crystallographic analysis

The phytofabricated CuONPs were shiny black in color. The structure and crystallinity of CuONPs fabricated from WGLLE had been examined by XRD patterns as shown in figure 3. A powder XRD was carried out using monochromatic CuKα1 28radiation (wavelength 1.5406 A°), in the angular range 2θ of 200-800 operating at a voltage of 40 kV and a current 40 mA. XRD profile analysis revealed a series of prominent diffraction peaks at 32.48°, 35.54°, 38.72°, 48.8°, 53.48°, 58.32°, 61.58°, 68.6°, 72.38° and 75.16° which corresponds to (110), (002), (111), (20-2), (020), (202), (11-3), (220), (311) and (004) sets of planes respectively. Also, some unidentifiable peaks can be seen attributed to some organic content or amorphous impurities. The observed sets of planes are indexed based on the monoclinic structure of CuO by comparing the data from JCPDS card No. 48- 1548. Due to the monoclinic structure of CuO, the XRD profile analysis thus clearly illustrated that the phytogenically synthesized CuONPs are good crystalline in nature with high purity. The particle size (average) of phytogenically synthesized CuONPs was 40 ± 0.5 nm, calculated using Debye-Scherrer's formula [22-28].

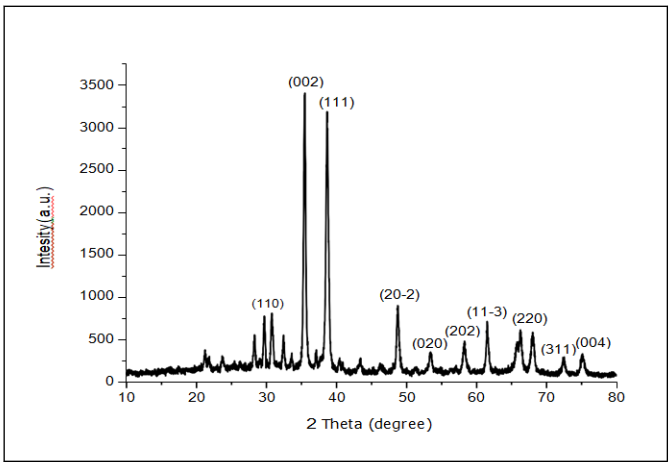

Figure 3: XRD pattern of WGLLE mediated CuONPs.

Vibrational properties

FTIR spectrum of WGLLE mediated CuONPs is represented in figure 4. The broad peak at 3840 cm^{-1} is credited to the stretching vibration of aromatic phenolic (-OH) compounds. The bands at 3242 cm^{-1} can be allied with asymmetric stretching of the C-H band of alkanes. The peak assigned at 1687 cm^{-1} is due to the carbon-carbon double bond stretching frequency of polyphenol confirming the aromatic compounds. The peaks at 619 cm^{-1} and 518 cm^{-1} prove the formation of metal oxide *i.e.,* Cu-O, resulted of Cu-O bond stretching [29]. The FT-IR results support the existence of biomolecules as detected by phytochemical screening.

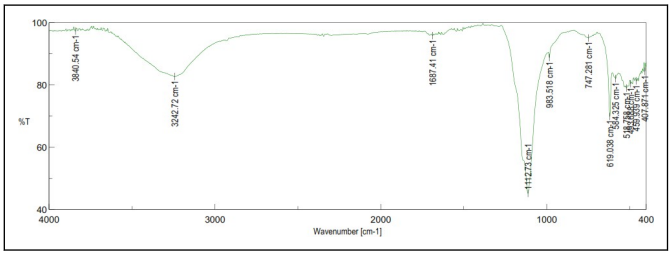

Figure 4: FTIR spectra of CuONPs.

FESEM-EDAX study

The intention of this analysis was to decide the structure along with the morphology of synthesized material. The FESEM images in figure 5 supports the XRD analysis as particle size range from 30 nm to 95 nm with a quasi-spherical shape.

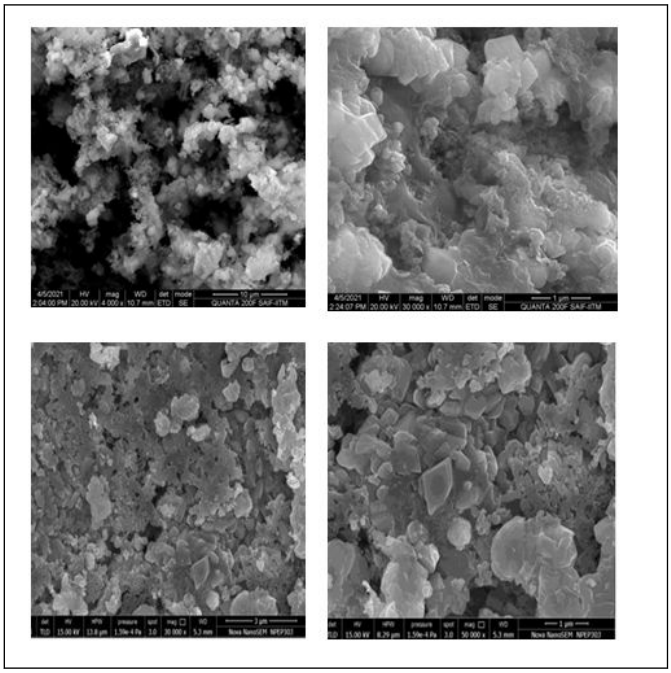

Figure 5: FESEM images of CuONPs.

The purity and chemical constituents of CuONPs were depicted by EDAX spectra shown in Figure 6, which state that, the CuONPs are comprised of mainly Cu and O along with other elements S, K, C, Mg, Si, and P attributed to biomolecules associated with CuONPs stating crystallinity of the synthesized nanomaterial [30].

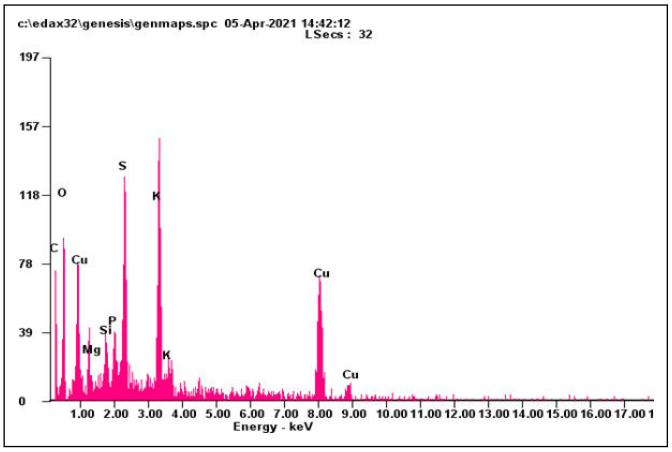

Figure 6: EDAX spectrum of CuONPs.

HRTEM analysis

Figure 7 shows proof of the non-aggregated spherical, crystalline, and monoclinic nature of WGLLE- mediated CuONPs. The particle size ranges between 2-50 nm, well in agreement with XRD study.

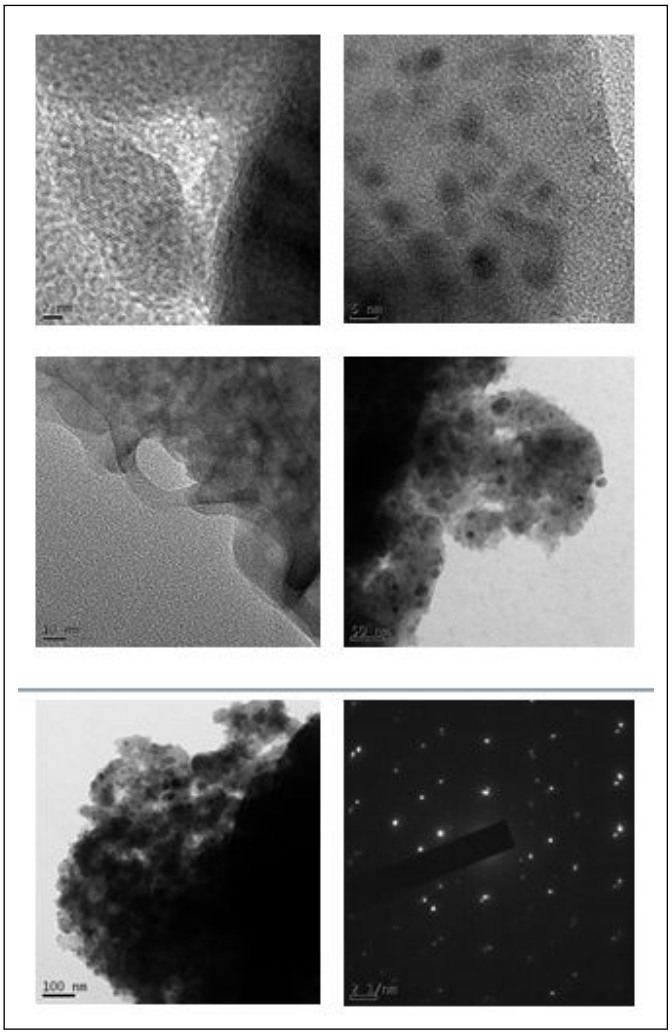

Figure 7: HRTEM images and SAED pattern of CuONPs.

UV-Visible study

The wavelength of 200-800 nm was the range to record the UV-Visible spectra of CuONPs as depicted in figure 8. The absorbance around 300 nm is a clear indication of the establishment of CuONPs, attributed to the charge transition from valence band to conduction band (O^{2-} to Cu^{2+}ion).

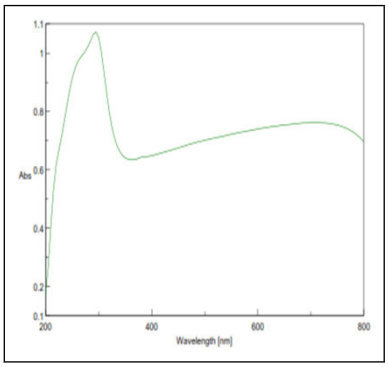

Figure 8: UV-Visible spectra of CuONPs.

Photoluminescence study

The PL spectrum was recorded in the 280-601 nm range. Figure 9 shows the luminescence character of WGLLE mediated CuONPs as the emission bands appear at 295 nm and 590 nm indicating green-yellow emission at an excitation wavelength of 290 nm. The first peak is attributed to band edge emission while the second one corresponds to the artefact. Further, the stokes pattern can be observed as the emission peak at 579 nm is 2-fold of excitation wavelength *i.e.,* 290 nm [8].

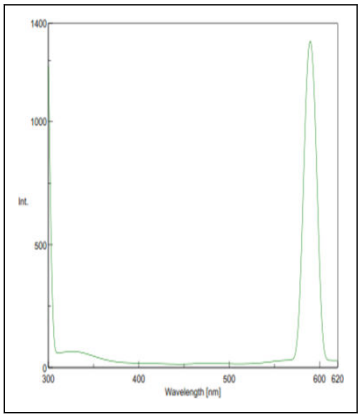

Figure 9: PL spectra of synthesized CuONPs.

Phytochemical screening of WGLLE

Table 1 represents the biomolecules existing in the WGLLE. These important phytochemicals are capable to act as natural reducing cum capping agents in the eco benign synthesis of CuONPs [31]. Further, the existence of these biomolecules had been confirmed by FT-IR spectra. Figure 10 shows important molecules reported in WGLLE.

Phytoconstituents	Test results
Flavonoids	P
Phenols	P
Steroids	P
Alkaloids	Ab
Tannins	Ab
Glycosides	P
Terpenoids	P
Quinones	Ab

Table 1: Phytochemical testing of WGLLE

P- Presence of phytoconstituents, Ab- Nonappearance of phytoconstituents

Possible Growth Mechanism of CuONPs

The molecules representing figure 10 are considered for working as natural stabilizing and reducing agents in the phytofabrication of CuONPs [32].

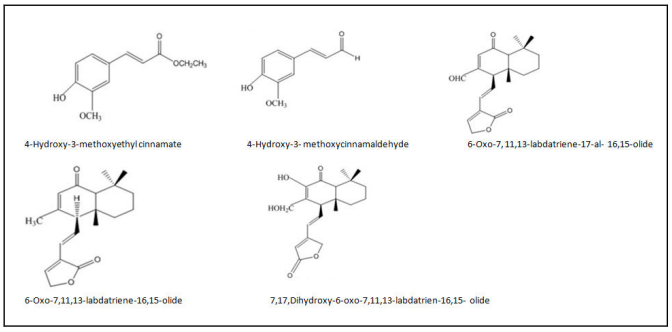

Figure 10: Important biomolecules in WGLLE.

Growth Mechanism

Figure 11 represents the possible growth mechanism of CuONPs. Initially, active site of WGLLE gets bound with Cu^{2+} which later being reduced to Cu0. This Cu0 on oxidation leads to CuONPs.

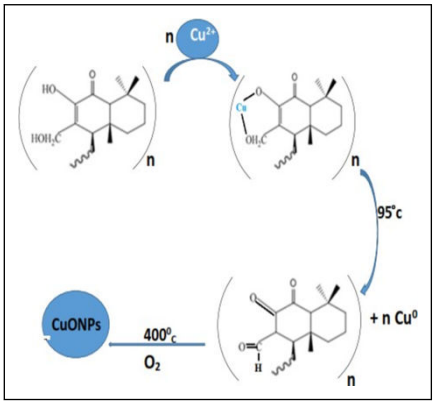

Figure 11: Plausible mechanism of growth of CuONPs.

Antibacterial activity

The antibacterial efficiency of the WGLLE-led CuONPs is tabulated in table 2. The CuONPs showed outstanding antibacterial activities *vs E. coli* and *S. Pyogenus* and reasonable bactericidal properties *vs S. Aureus* and *P. Aeruginosa* concerning reference drug Ampicillin.

Test Pathogens	MIC(µg/ml) of CuONPs	MIC(µg/ml) of Ampicillin	MIC(µg/ml) of Ciprofloxacin
S. Aureus (MTCC-96)	250	250	50
E. coli (MTCC-443)	100	100	25
P.Aeuruginosa (MTCC-1688)	250	100	25
S. Pyogenus (MTCC-442)	125	100	50

Table 2: MIC of CuONPs against bacteria

Antifungal activity

The antifungal efficacy of CuONPs phytofabricated from WGLLE is shown in table 3. The fungal strains *Aspergillus niger* and *Aspergillus clavatus* showed reasonable antifungal activities while the *Candida albicans* showed lower activity *vs* CuONPs concerning Griseofulvin and Nystatin as reference drugs.

Test Pathogens	MIC(µg/ml) of CuONPs	MIC(µg/ml) of Graseofulvin	MIC(µg/ml) of Nystatin
C.albicans (MTCC-227)	1000	500	100
A.niger (MTCC-282)	500	100	100
A.clavatus (MTCC-1323)	500	100	100

Table 3: MIC of CuONPs against fungi

Photocatalytic activity

The photocatalytic activities of CuONPs were tested towards photodegradation of MB under sunlight using 1.0 g/dm^3 of CuONPs. Figure 12 and 13 shows the decreasing concentration of MB *vs* time.

The decomposition rate of dye concentration *vs* irradiation time is presented in figure 14. Initially, the blank experiment was conducted without adding a photocatalyst (photolysis). The degradation rate without catalyst was negligible but on adding photocatalyst, the concentration of the MB gradually decreased under the sunlight and 100% degradation was achieved after 70 minutes.

The optimization of catalyst amount from 0.1 to 1.0 g/ dm^3 helped to achieve 100% degradation in 70 minutes. But a further increase in the amount of photocatalyst above 1.0 g/dm^3 decreased the efficiency, attributed to the aggregation of photocatalyst [33].

The table 4 displays the comparison of photocatalytic potency of CuONPs with reported literature [34-36]. The data reveals the superiority of WGLLE-mediated CuONPs as a photocatalyst.

Sr.No.	Materials	Plant used	Dye Pollutant	Irradiation source	Degradation time (Min)	Degradation Efficiency (%)	References
1	CuONPs	*Leucophyllum frutescens*	Methylene Blue	Sunlight	120	88%	[34]
2	CuONPs	*Bergenia ciliata*	Methylene Blue	Sunlight	135	92-85%	
3	CuONPs	*Elaeagnus indica*	Methylene Blue	Sunlight	360	76%	[35]
4	CuONPs	*Camellia sinesis*	Methylene Blue	Sunlight	180	85.50%	[36]
5	CuONPs	*Prunus africana*	Methylene Blue	Sunlight	180	83.20%	[36]
6	CuONPs	*Hedychium coronarium Koenig*	Methylene Blue	Sunlight	70	100%	Present Work

Table 4: Comparison of photocatalytic efficacy of phyto fabricated CuONPs with recent literature

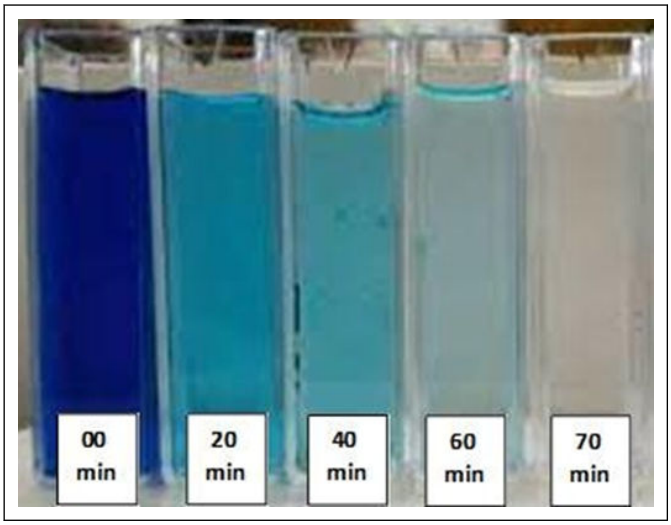

Figure 12: Images of photodegradation of MB with respect to time.

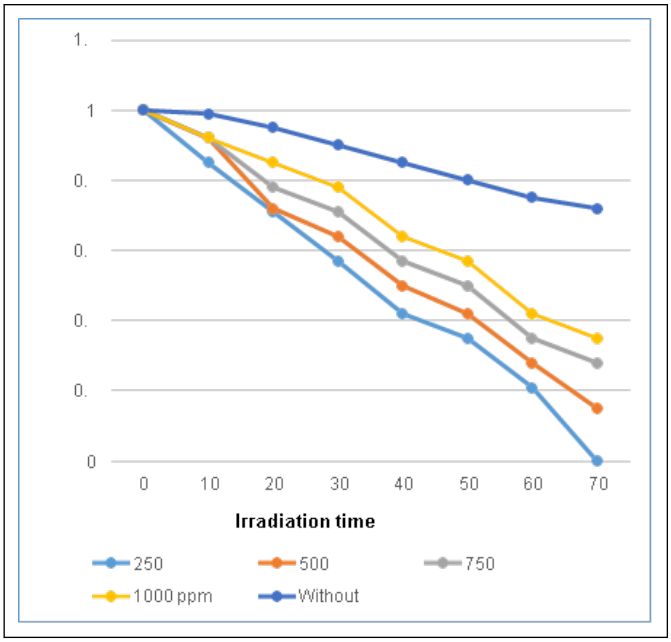

Figure 13: A plot of A/A0 with time for the photodegradation of MB.

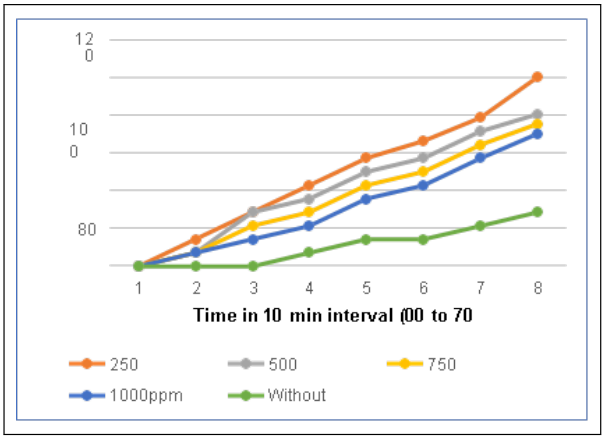

Figure 14: Rate of decomposition of MB by using CuONP.

Conclusion

The present article has been devoted to synthesizing CuONPs using WGLLE. The method reported for synthesis follows green chemistry ethics leading to an eco-balancing, sustainable and simple pathway. The synthesized CuONPs were characterized using basic and modern analytical tools like UV-Visible spectra, XRD, FTIR, FESEM-EDAX, HRTEM, and PL, *etc.,* and exhibited excellent antibacterial activities with reasonable antifungal potency against selected bacterial and fungal pathogens. This can lead to the development of antibacterial drugs while luminescent character can turn useful in optical materials, after a detailed investigation.

Moreover, 100% degradation of MB was achieved within 70 min. using novel CuONPs under sunlight. This indicates that this material can be a very good photocatalyst for the detoxification of MB dye.

Data Availability Statement

Data will be made available with a reasonable request.

Author Contribution

PBN put forth the idea, and PBN, AJG, and KGM carried out the laboratory work. APS helped in the identification of the plant. PBN and KGM wrote the manuscript and finalized it concern with the other two.

Acknowledgment

The authors are grateful to Instrumentation Centre, P.A.H. Solapur University, Solapur, CRNTS, IIT Bombay, IIT Madras, Jaysingpur College Jaysingpur, and Microcare Lab., Gujarat for the support in technical, instrumental, and biological activities.

Conflict of Interest

The authors do not have any conflict of interest.

References

1. Steffanie AS, Sally CD, Jasmine RM (2020) Confronting antimicrobial resistance beyond COVID-19 pandemic and US election. Lancet 396: 1050-1053.
2. Neill JO (2016) Tackling drug resistant infections globally: Final report and recommendations. Government of the United Kingdom, United Kingdom, Europe.
3. Vijayraghavan K, Ashokkumar T (2017) Plant-Mediated biosynthesis of metallic nanoparticles: A review of literature, factors affecting synthesis, characterization techniques and applications. J Environ Chem Eng 5: 4866-4883.
4. Gregory M, Karthik S, Qaisar M, Rajendran KS, Dariusz K, et al. (2018) Secondary metabolites in the green synthesis of metallic nanoparticles. Materials 11: p940.

5. Suresh G, Harshal D, Pawan T, Vijay M (2021) Plant -based green synthesis and applications of cuprous oxide nanoparticles. Handbook of Greener Synthesis of nanomaterials and compounds 2: 201-208.

6. Trupti P, Suresh G, Khanderao P, Shreyas P, Rajeshwari O (2021) Phytogenic synthesis of manganese dioxide nanoparticles using plant extracts and their biological application. Handbook of greener synthesis of nanomaterials and compounds 2: 209-218.

7. Suresh G, Khanderao P, Shreyas P, Ananda HCM, Rajeshwari O (2021) Biosynthesis of silver sulfide nanoparticles and its applications. Handbook of greener synthesis of nanomaterials and compounds 2: 191-200.

8. Pansambal S, Deshmukh K, Savale A, Ghotekar S, Pardeshi O, et al. (2017) Phytosynthesis and biological activities of fluorescent cuo nanoparticles using Acanthospermum hispidium l. extract. Journal of nanostructure 7: 165-174.

9. Venkata RCh, Neelkanta IR, Ravindranadh K, Raghava KR, Nagaraj PS (2020) Copper-doped zro2 nanoparticles as high- performance catalysts for efficient removal of toxic organic pollutants and stable solar water oxidation. J Environ Manage 260: p110088.

10. Gawande M B, Goswami A, Felpin F X, Asefa T, Huang X, et al. (2016) Cu and Cu based nanoparticles: Synthesis and applications in catalysis. Chem Rev 116: 3722-3811.

11. Mohsenzadeh S, Karimi J (2015) Rapid, green, and eco-friendly biosynthesis of copper nanoparticles using flower extract of aloe vera. Syn React Inorg Met 45: 895–898.

12. Kolekar R, Bhade S, Kumar R, Reddy P, Singh R, et al. (2015) Biosynthesis of copper nanoparticles using aqueous extract of eucalyptus sp. plant leaves. Curr Sci, Mumbai, India.

13. Rajivgandhi G, Maruthupandy M, Muneeswaran T, Ramachandra G, Manoharan N, et al. (2018) Biogenically synthesized copper oxide nanoparticles enhanced intracellular damage in ciprofloxacin-resistant ESBL producing bacteria. Microb Pathog 127: 267-276.

14. Imran MD, Farhan A, Zaib H, Maria M (2017) Green adeptness in the synthesis and stabilization of copper nanoparticles: Catalytic, antibacterial, cytotoxicity, and antioxidant activities. Nanoscale Res Lett 12: p638.

15. Bisht S, Bisht NS, Bhandari S (2012) In vitro plant regeneration from seedling explants of hedychium coronarium j. koenig. J Mol Pl Res, Uttarakand, India.

16. Fransworth NR (1996) Biological and phytochemical screening of plants. J Pharm Sci 55: 225-227.

17. Wiegand I, Hilpert K, Hancock REW (2008) Agar and broth dilution methods to determine the Minimal Inhibitory Concentration (MIC) of antimicrobial substances. Nature Protocols 3: 163-175.

18. Zinab MA, Hamid RR, Ali M, Asad M (2019) Ultrasonic and microwave assisted extraction as rapid and efficient techniques for plant mediated synthesis of quantum dots: green synthesis, characterization of zinc telluride and comparision study of biological activities. New J Chem 43: 15126-15138.

19. Prashansa S, Suman P, Vivek D, Kajal T, Veera S, et al. (2019) Green synthesis and characterization of copper nanoparticles by tinospora cardifolia to produce nature-friendly copper nano-coated fabric and their antimicrobial evaluation. J Microbiol Methods 160: 107-116.

20. Apoorva M, Sonika J, Dharma K, Vivek D, Raghava KR, et al. (2019) A facile one pot synthesis of novel pyrimidine derivatives of 1,5benzodiazepines via domino reaction and their antibacterial evaluation. J Microbiol Methods 163: p105648.

21. Patterson AL (1939) The scherrer formula for x-ray particle size determination. Phys Rev 56: 978-982.

22. Mane KG, Nagore PB, Pujari SR (2018) Synthesis, photophysical, electrochemical and thermal investigation of anthracene doped 2-Naphthol luminophors and their thin film for optoelectronic devices. J Fluoresc 28: 1023-1028.

23. Mane KG, Nagore PB, Pujari SR (2019) Synthesis of highly fluorescent D-A based p-Terphenyl Luminophors and their thin films for optoelectronic applications. J Fluoresc 29: 1001-1006.

24. Mane KG, Nagore PB, Pujari SR (2019) Novel 2-naphthol luminophors for optoelectronics. Appl Phys A 125: p729.

25. Mane KG, Nagore PB, Pujari SR (2019) Synthesis of novel blue and green light emitting 4-Nitrophenol luminophors for optoelectronics. J Fluoresc 29: 1371-1380.

26. Mane KG, Nagore PB, Pujari SR (2020) Photophysical and structural aspects of perylene doped 2-naphthol luminophors: Green emission by exciplex formation. Luminescence 35: 292-298.

27. Pujari SR, Nagore PB, Ghoti AJ, Mane KG (2021) Novel donor-acceptor based 2-Naphthol luminophors as hole-transporting materials for optoelectronics. Journal of Fluorescence 31: 259-267.

28. Sone BT, Diallo A, Fuku XG, Fakim AG, Maaza M (2017) Biosynthesized CuO nano-platelets: Physical properties and enhanced thermal conductivity nanoflidics. Arab J Chem 5: p128.

29. Chandan T, Indranirekha S, Moushumi H, Manash RD (2014) Reduction of aromatic nitro compounds catalyzed by biogenic CuO nanoparticles. RSC Adv 4: 53229-53236.

30. Siddiqui H, Qureshi MS, Haque FZ (2014) One-step, template- free hydrothermal synthesis of CuO tetrapods. Optik 125: 4663-4667.

31. Gawade VV, Gavade NL, Shinde HM, Babar SB, Kadam AN, et al. (2017) Green synthesis of ZnO nanoparticles by using calotropis procera leaves for the photodegradation of methyl orange. J Mater Sci: Mater Electron 28: 140033-140039.

32. Bhosale RR, Pujari SR, Muley GG, Patil SH, Patil KR (2014) Solar photocatalytic degradation
of methylene blue using doped TiO2 nanoparticles. Solar Energy 103: 473–479.

33. Awais A, Mariam K, Safia K, Rafael L, Khamael MA, et al. (2022) Bio-Construction of CuO nanoparticles using texas sage plant extract for catalytical degradation of methylene blue. Journal of Molecular Structure 1256: p132522.

34. Gozde KA, Kanika D, Chauhan PK, Parveen C (2022) Multifunctional CuO nanoparticles with enhanced photocatalytic dye degradation and antibacterial activity. Research Square 32: 1-15.

35. Indira D, Krishnamoorthy M, Ameen F, Ahmad SB, Amurgum K, et al. (2022) Biomimetic facile synthesis of zinc oxide and copper oxide nanoparticles from elaeagnus indica for enhanced photocatalytic activity. Environmental Research 212: p113323.

36. Kenneth S, Denis KB, Martin KA, Eddie MW, Francis E (2022) Phyto-Mediated copper oxide nanoparticles for antibacterial, antioxidant and photocatalytic performances. Front Bioeng Biotechnol 10: p820218.